Study of ion emission from a germanium crystal surface under impact of fast Pb ions in channeling conditions

A. L'hoir, Charbel Koumeir, S. Della Negra, P. Boduch, P. Roussel-Chomaz, A. Cassimi, Marius Chevallier, C. Cohen, D. Dauvergne, M. Fallavier, et al.

Study of the ion emission from a germanium crystal surface under impact of fast Pb ions in channeling conditions

A. L'Hoir [a,*], C. Koumeir [b], S. Della Negra [c], P. Boduch [d], P. Roussel-Chomaz [e], A. Cassimi [d], M. Chevallier [b], C. Cohen [a], D. Dauvergne [b], M. Fallavier [b], D. Jacquet [c], B. Manil [d], J-C. Poizat [b], C. Ray [b], H. Rothard [d], D. Schmaus [a], M. Toulemonde [d].

[a] Institut des NanoSciences de Paris, Université Pierre et Marie Curie-Paris 6, UMR7588 CNRS, 140 rue de Lourmel 75015 Paris, France.
[b] Institut de Physique Nucléaire de Lyon, Université de Lyon, Université Lyon 1, CNRS/IN2P3, 4 rue Enrico Fermi, 69622 Villeurbanne, France.
[c] Institut de Physique Nucléaire d'Orsay, Université Paris-Sud 11, CNRS/IN2P3, 91406 Orsay, France.
[d] Centre de Recherche sur les Ions, les Matériaux et la Photonique, UMR 6637 CNRS-CEA, rue Claude Bloch, 14040 Caen, France.
[e] GANIL, BP 55027, 14076 Caen Cedex 5, France.

*Corresponding autor. *Email adress:* alain.lhoir@insp.jussieu.fr. Phone: 33 (0) 1 44 27 31 61. Fax: 33 (0)1 44 27 47 11.

Keyword: Channeling; Sputtering; Ion emission; Heavy ions; Electronic energy deposition; Charge state; Transverse energy.

Abstract.

A thin germanium crystal has been irradiated at GANIL by Pb beams of 29 MeV/A (charge state Q_{in} = 56 and 72) and of 5.6 MeV/A (Q_{in} = 28). The induced ion emission from the sample entrance surface was studied, impact per impact, as a function of Q_{in}, velocity v_{in} and energy loss ΔE in the crystal. The Pb ions transmitted through the crystal were analyzed in charge (Q_{out}) and energy using the SPEG spectrometer. The emitted ionized species were detected and analyzed in mass by a Time of Flight multianode detector (LAG). Channeling was used to select peculiar ΔE in Ge and hence peculiar Pb ion trajectories close to the emitting entrance surface. The experiment was performed in standard vacuum. No Ge emission was found. The dominating emitted species are H^+ and hydrocarbon ions originating from the contamination layer on top of the crystal. The mean value <M> of the number of detected species per incoming Pb ion (multiplicity) varies as $(Q_{in}/v_{in})^p$, with p values in

agreement with previous results. We have clearly observed an influence of the energy deposition ΔE in Ge on the emission from the top contamination layer. When selecting increasing values of ΔE, we observed a rather slow increase of $<M>$. On the contrary, the probabilities of high multiplicity values, which are essentially connected to fragmentation after emission, strongly increase with ΔE.

I. Introduction.

When a swift heavy ion beam penetrates into a crystal parallel to a major axis, most of the ions follow trajectories steered by the repulsive potential of strings and, for not too large depths, their transverse energy $E_\perp$ (kinetic plus potential energy) associated to the ion motion in the plane perpendicular to the beam direction (transverse plane) is conserved: particles are channeled [1].

Particles penetrating into a crystal very close to a string (at a distance of the order of the thermal vibration amplitude), get a very high $E_\perp$ value. They suffer successive correlated elastic collisions with the target nuclei of the string, that govern trajectories. They also suffer inelastic collisions on the target electrons, mainly core electrons, leading, in the surface region, to a very high energy loss $dE/dx = S_{in}(E_\perp)$ which may be at least one order of magnitude larger [1-4] than the stopping power S_R for a random orientation of the crystal (or for an equivalent amorphous target). At a very short time scale (typically 10^{-17} s), the successive atoms of the string are highly ionized and, depending on the kinetics of the crystal neutralization, these ions may repel each other, leading to a Coulomb explosion of the string close to the surface. This could possibly lead to a strong ion emission from the crystal for such high $E_\perp$ incident ions. On the contrary, particles penetrating into the crystal far from the rows (of low $E_\perp$), suffer a small $S_{in}(E_\perp)$ value (typically $S_{in}(E_\perp) = 0.4 \times S_R$ [3]) and ion emission is expected to be much smaller than for high $E_\perp$ values or for random incidence conditions.

As will be shown in this paper, a precise $E_\perp$ selection is achievable in a transmission type experiment with a thin crystal by selecting the outgoing charge state Q_{out} and/or the total energy loss $\Delta E(Q_{out})$. However, for studying ion emission from a crystal as a function of the energy loss close to the surface, an *Ultra-High Vacuum* system coupled to a high energy heavy ion accelerator would be necessary. Under such conditions, the residual contaminants would have been reduced to adsorbate gases like H_2 or CO_2 [5].

The first stage experiment presented in this paper was performed under *standard vacuum* in the SPEG beam line [6] at GANIL (Caen). We used a thin

(100) germanium crystal and the beam was aligned along the [110] direction (total path length 0.85 μm). Both faces of the crystal were unavoidably covered by a thin disordered layer, containing essentially H, O, C and Ge atoms (see below). In the last decades, numerous studies ([7-8]) were devoted to the emission of organic compounds as a function of the beam charge state Q_{in} (i.e. as a function of the energy loss rate), in particular when Q_{in} is far from the equilibrium charge state Q_{eq} in the solid. In the latter case, a fast variation with depth z of Q towards Q_{eq} permits to observe the so called "depth effect" [7] characterized by a mean depth $<z_d>$ (typically 1-15 nm) within which the interaction of ions with the solid has an influence on the surface desorption.

In the present experiment, for a given incident ion beam (i.e. given Q_{in}, v_{in}, charge changing cross sections), we use channeling in transmission to select various energy depositions in the very near surface region of the Ge crystal below the disordered layer: one of the main aims of our experiment is then to study ion emission as a function of the stopping power $S_{in}(E_\perp)$ in this region. As already underlined, channeling allows to select $S_{in}(E_\perp)$ values varying over more than one decade. In the present experiment, Ge ion emission is not expected to be the dominant process: ion emission is expected to originate from the entrance disordered top layer. Note also that ion emission represents only a small fraction of the sputtering yield Y (high proportion of neutral species) and may not be representative of the overall emission.

Three lead ion beams (Z = 82) were used:
i) 29 MeV/A Pb^{72+} and *ii)* 29 MeV/A Pb^{56+}. At this energy, the mean equilibrium charge state Q_{eq} is very close to 72 (see table 1); *iii)* 6.5 MeV/A Pb^{28+} (Q_{eq} = 55). The random stopping power S_{Req} of germanium at charge equilibrium [9] for 6.5 MeV/A and 29 MeV/A Pb are close to each other (see table 1). 29 MeV/A Pb^{56+} and 6.5 MeV/A Pb^{28+} ions being far from charge equilibrium, S_{in} differs markedly from S_{Req}, even in random geometry. Roughly one can assume that S_{in} varies like $\zeta_{in.} = (Q_{in}/v_{in})^2$. One gets similar values for the Pb^{56+} and Pb^{28+} beams (see table 1). The corresponding value is about 60% higher for the 29 MeV/A Pb^{72+} beam.

In addition to the information brought specifically by channeling measurements, the results obtained with the three different ion beams in random geometry provide, like in previous studies [7], information on the dependence of ion emission on Q_{in}, v_{in}, and on the trend towards charge equilibrium.

II. Experimental conditions.

II.1 Crystal

The (100) Ge crystal, provided by the Aarhus University (Denmark), was obtained by epitaxial growth on a Si crystal followed by electrochemical dissolution of Si. In order to remove the defects induced by the lattice mismatch at the Ge/Si interface, the sample was annealed under standard vacuum at 900 K during 5 h. The Ge surface cleaning was performed using HF at 20% during 3 min [10-11] just before putting the sample into the vacuum chamber.

The surface disordered layer was chemically analyzed by Rutherford Backscattering Analysis (RBS) and Nuclear Reaction Analysis (NRA) at the 2.5 MV Van de Graaff accelerator of INSP. We measured the quality of the crystal and the absolute amount of Ge in the surface disordered layer using channeling and RBS. The absolute amount of C and O was obtained using the C^{12}(d,p) and O^{16}(d,p) nuclear reactions [12]. We found about 5×10^{15} cm^{-2} C and O atoms in the layer. The Ge surface peak observed in the RBS-channeling measurements indicates that the Ge atoms displaced from crystallographic sites amount to about 3×10^{15} cm^{-2}. These atoms thus likely form a thin disordered oxide layer of GeO_2 stoichiometry. The C atoms come from a hydrocarbon layer on top of this oxide. The minimum RBS yield χ_{min} along [110], integrated over the whole crystal thickness is 0.043, with a low 0.025 value close to the entrance surface, indicating a good crystalline quality of our sample after thermal annealing.

II.2 Experimental set-up at GANIL

The (100) Ge crystal was mounted on a 3-axis goniometer (see figure 1), controlled with a 0.05 mrad precision. The crystal is tilted at 45° for [110] alignment and its potential is + 8 kV relative to ground. The secondary electrons ejected from the exit surface are accelerated towards a Micro Channel Plates (MCPs) electron detector, set at +12 kV. Although the absolute electron yield has been used previously by us to characterize the transverse energy of channeled ions [13], this detector was here simply used to provide a START signal for each ion entering the crystal.

The transmitted beam was analyzed by the SPEG high resolution spectrometer (described in [6]). For each outgoing charge state Q_{out}, the projectile energy spectrum $G(Q_{out}, E_{out})$ was measured, with a 2×10^{-4} resolution. Typical relative energy losses $\Delta E/E$ range from 3×10^{-3} to 2×10^{-2}.

A Time Of Flight (TOF) Multianode system, called LAG, located at 45° to the beam and [110] direction, analyzes the positive ions emitted from the entrance surface of the Ge crystal. It is provided with an accelerating grid close to the crystal, set at -2 kV. This detector is made of a set of three MCPs (Ø=42mm, geometrical efficiency 0.6) and of a 64 pixels anode array of 1600

mm^2 (MCPs detectors are used to deliver STOP signals). A similar detector with 256 anodes is described in reference [14]. With this detector located at 400 mm from the target one measures the mass of the ions emitted from the target by means of their time of flight, the number of ions emitted simultaneously and, if necessary, the angular distribution of these ions. For each incident projectile, the pixilated detector records the total number of impacts on the detector (multiplicity M). The TOF detection efficiency for secondary ions in the mass range from 1 to 300 a.u. is η, ranging between 0.44 and 0.49. This efficiency accounts for the MCPs geometrical efficiency and the pixel structure of the anode array [15]. The emission yields given throughout this paper are not corrected for the detector efficiency and should not be considered as absolute values.

The TOF measurement cannot give the axial velocity of the secondary ions when emitted, but the angular distributions of the ions accelerated from the target can be deduced from the 2D position spectra delivered by the multipixel detector in coincidence with windows set on the TOF peaks [15]. The LAG mass resolution varies from 0.1 to 0.25 atomic mass unit (amu), depending on the mass and the detected species.

The GANIL beam intensity was kept very low, about 10^3 ions/second. This permits an ion-by-ion analysis: Q_{out}, ΔE, emitted masses (and their 2-D position on the LAG) are simultaneously recorded.

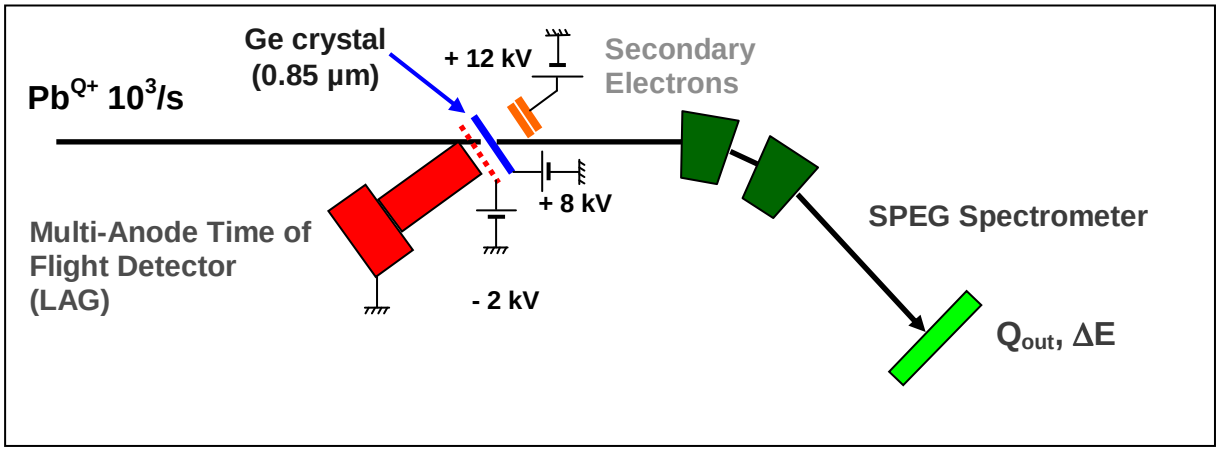

Figure 1(color on line): experimental set-up

III. Results

III.1 Energy loss measurements in SPEG

Energy loss spectra were recorded in SPEG for each Q_{out}. Typical energy loss spectra are displayed in figure 2 for a 29 MeV/A Pb^{72+} beam. Here $Q_{out} = Q_{in} = 72$. In this figure, the direct beam and the energy loss spectrum for a random beam orientation are compared to the [110] aligned beam spectrum $G(Q_{out} = 72, \Delta E)_{[110]}$. The random orientation was set at 0.6° from the axial direction, i.e. at a much larger angle than the critical channeling angle (0.1°). For [110] alignment, $Q_{out} = 72$ represents 70% of the overall beam (and 30% for the random orientation). The aligned energy loss spectrum is broad, reflecting the various trajectories in the crystal. High ΔE values correspond high $E_{\perp}$ ions that enter the crystal very close to the [110] rows. The highest measured energy losses correspond to more than 2 times the mean energy loss ΔE_R for a random orientation. In fact, ΔE corresponds to the energy loss of the ions all along their oscillating trajectories between the [110] rows. At the crystal entrance and, depending on the oscillations, in a few places in the crystal bulk, ions interact with the [110] rows at grazing incidence. In this region, the stopping power is much greater than S_R. But for most of their path, the ions travel rather far from the rows, where the stopping power is smaller than S_R. Hence, trajectories leading to a total energy loss $\Delta E > 2\Delta E_R$ correspond to S_{in}/S_R much larger than 2 close to the surface: selecting ΔE in the $G(Q_{out} = 72, \Delta E)_{[110]}$ distribution gives access to variations of S_{in} over a very wide range (typically one order of magnitude).

Similar energy spectra were recorded for the three Pb ion beams used in our experiment, together with the charge state distributions $F(Q_{out})$ of the transmitted beam, in random and aligned geometries.

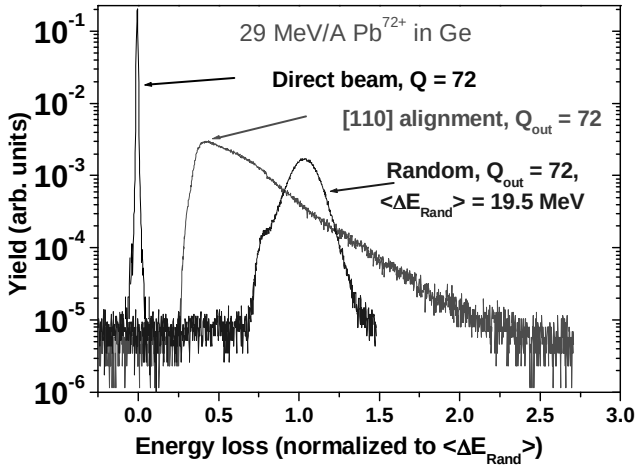

Figure 2 (color on line): Energy loss distribution of the transmitted ions as measured by the SPEG spectrometer for a 29 MeV/A Pb^{72+} incident beam: direct beam (crystal target removed), energy spectrum of ions transmitted

through the Ge crystal (0.85 μm) for a random orientation of the crystal and for the emerging charge state $Q_{out} = Q_{in} = 72$; corresponding spectrum for the beam aligned with the [110] direction.

III.2 Ion emission measurements with LAG

III.2.1) Mass spectrum

For each Pb ion impact on the target entrance surface, one measures with the LAG the number M (multiplicity) and the corresponding masses *m* of all the detected species consecutive to the emission of a positive ion. A mass spectrum as measured by the LAG is shown in figure 3 for a 6.5 MeV/A Pb^{28+} ion beam incident on the Ge crystal randomly oriented. It was recorded for $53 \leq Q_{out} \leq 57$ (i.e. most of the transmitted beam; in fact the mass distribution is almost independent of Q_{out} in random and [110] alignment). As expected [16-18] a very high H^+ yield is observed. Considering the isotopic composition of Ge and the corresponding masses (around 72 amu), one finds that there is no evidence for Ge ion emission. Thus the mass spectrum originates essentially from the hydrocarbon top layer.

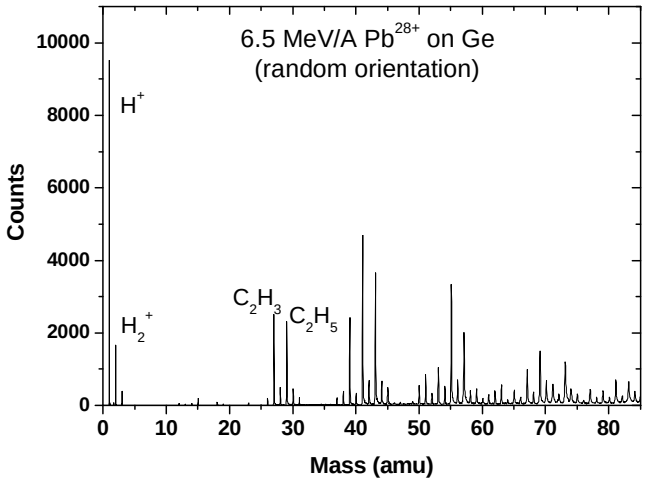

Figure 3: mass distribution of ion species emitted by the entrance face of the Ge crystal (random orientation) under 6.5 MeV/A Pb^{28+} bombardment as measured by the LAG.

III.2.2) Multiplicity

For each Pb ion impact, the number M of detected ions in the LAG is a random variable with possible values $n = 0,1,2$ etc…, associated probabilities P_o, P_1, P_2

etc… and mean value $\langle M \rangle = \Sigma_n nP_n$. In our ion-by-ion experiment, for a given bombarding ion, we may determine the P_n associated to given Q_{out} and ΔE values. M corresponds here to the overall ion emission, whatever the emitted mass. We may also measure the emission yield for given masses or group of masses (light, heavy etc…)

***a)* Multiplicity mean value.**

We have measured <M> in random and aligned geometries with very high statistics. We have obtained the following results (see table 1) with no selection on ΔE, and with Q_{out} in a range corresponding to most of the transmitted beam.

Ion Q_{in}, E_{in}	Q_{eq}	S_{Req} (keV/nm)	$\zeta_{in}=(Q_{in}/v_{in})^2$ (a.u.)	$\langle M \rangle_R$	$\langle M \rangle_{[110]}$
6.5 MeV/A Pb^{28+}	55	35	3.0	0.68	0.82
29 MeV/A Pb^{56+}	71.5	27	2.7	0.79	0.83
29 MeV/A Pb^{72+}	71.5	27	4.6	1.72	1.80

Table 1: mean equilibrium charge state Q_{eq} (random orientation), equilibrium random stopping power S_{Req} [9], stopping parameter $\zeta_{in} = (Q_{in}/v_{in})^2$ (see §I; here v_{in} is expressed in Bohr velocity unit), multiplicity mean values for random ($\langle M \rangle_R$) and aligned ($\langle M \rangle_{[110]}$) geometries.

We observe that <M> depends on the crystal orientation but that this dependence is weak. Moreover, <M> is larger in the aligned geometry. This paradoxical feature will be discussed in section IV. <M> depends on the ion beam energy E_{in} (velocity v_{in}) and charge state Q_{in}. One finds that <M> scales approximately as $(Q_{in}/v_{in})^3$. If one assumes that the stopping power S_{in} for these ions scales as $\zeta_{in}.= (Q_{in}/v_{in})^2$, <M> is found proportional to $S_{in}^{1.5}$.

For a random orientation and the three ion beams, we have also measured the mean ion emission yield as a function of the mass *m* of the ejected species $\langle M(m) \rangle$. One finds that $\langle M(m) \rangle$ depends on the stopping power approximately as S_{in}^{p}. For very light masses *m*, one finds p = 2 to 3, whereas for very heavy masses, p = 1. Such differences were already pointed out in the literature [7], although desorption of surface adsorbates - which may be more weakly bound - may not be comparable in a straightforward way to high molecular weight organic layers. Detailed results on $\langle M(m) \rangle$ will be presented in a forthcoming publication.

b) Multiplicity distributions

As already indicated, the multiplicity mean value depends only very slightly on the crystal orientation. In fact, one of the main results in our experiment concerns the probability P_n associated with large multiplicity values (large n). Figure 4 gives the P_n distribution in random and in aligned geometries for 6.5 MeV/A Pb^{28+} incident ions. Thanks to the coincidences with SPEG, in all cases a background arising from ions impinging the grid could be suppressed. As for <M>, the random and [110] distributions are relatively close to each other at small n values. However, for $n > 6$, P_n is about two times larger for [110] than for the random orientation. This has little consequence on <M> since the corresponding P_n are small. Note that for the channeled beam (filled squares), there is here no selection on Q_{out} or ΔE. Among all the channeled ions, we now select two groups of particles:

i) The ions transmitted with high ΔE ($\Delta E > \Delta E_R$) and with high Q_{out} values (in the range $55 \leq Q_{out} \leq 57$ corresponding to the charges detected in random orientation conditions). These ions are representative of the ~ 5% ions with the highest $E_\perp$ in the transverse plane, i.e. that enter the crystal close to atomic strings.

ii) The ions transmitted with low ΔE and low Q_{out} ($38 \leq Q_{out} \leq 41$). They represent 4% of the transmitted beam and correspond to the best channeled ions in the beam.

With these two extreme selections, the channeled curve (filled squares) splits in two very different curves. First of all, the mean value <M> is nearly 5 times higher for the high ΔE than for the low ΔE selection. More strikingly, for $n > 5$, the probabilities P_n are nearly two orders of magnitude larger for the high energy loss trajectories (open squares) than for the low energy loss one (open circles). Moreover, also for high n, the P_n associated to high losses in [110] aligned geometry are one order of magnitude larger than for the random orientation. Note that for all these curves, the energy deposited in the disordered top layer is the same: the ion emission yield depends very strongly on the energy loss in the Ge crystal substrate, i.e. a depth effect does exist and extends over depths z_d larger than the disordered layer thickness. However, the mechanisms involved here in channeling geometry, may be somewhat different from the one involved in the depth effect described in [7] for a random geometry and large emitted molecules.

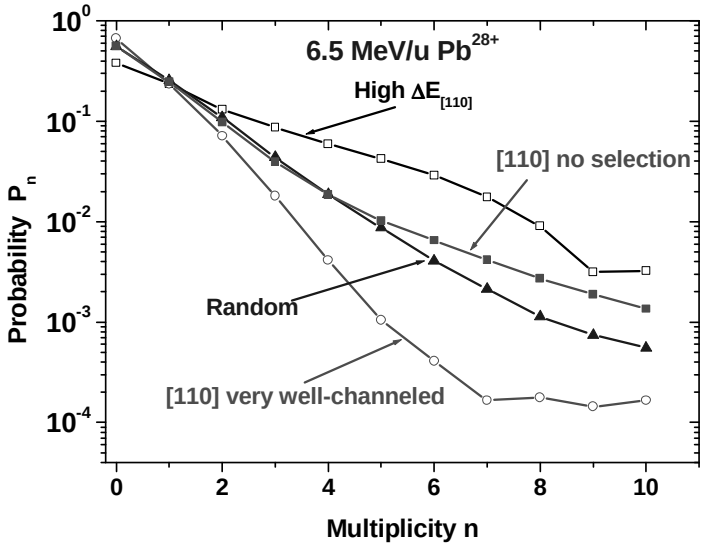

Figure 4 (color on line): Probability P_n for 6.5 MeV/A Pb^{28+} ions incident on the Ge crystal. The distributions are normalized to unity.

c) Multiplicity mean value and energy loss

The results on <M> given above in §III.2.2.*a)* were obtained without any selection on ΔE or Q_{out}. We have studied the variations <M(ΔE)> of the multiplicity mean value as a function of the total energy loss ΔE of the ions in the crystal. In particular (see figure 5), for the [110] energy loss spectrum of figure 2 (29 MeV/A Pb^{72+}), <M> varies linearly from 1.3 to 3.7 between the lowest ($0.3\times\Delta E_R$) and highest ($2.5\times\Delta E_R$) ΔE values. This variation of <M> with ΔE is steeper than one could have expected when considering the very small influence of channeling (see table 1) when no selection on ΔE is applied. On the other hand, as discussed in §III.1, to the lowest $\Delta E/\Delta E_R = 0.3$ value may correspond S_{in}/S_R close to 0.3 at the crystal entrance, but for $\Delta E/\Delta E_R = 2.5$, one may expect a much higher S_{in}/S_R ratio, of the order of 10: the variation rate of <M> with S_{in} is thus about 3 times smaller than the variation rate of <M> shown in figure 5.

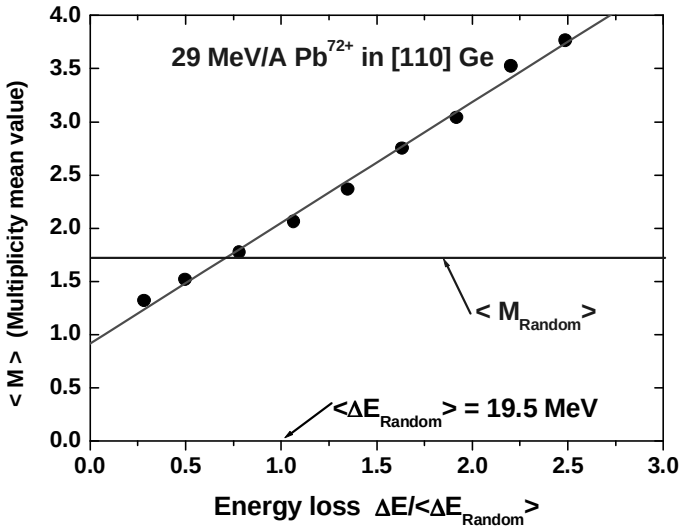

Figure 5 (color on line): Multiplicity mean value as a function of the total energy loss ΔE in the Ge crystal for 29 MeV/A Pb^{72+} incident ions (energy loss bins are selected in the [110] energy loss distribution of figure 2).

IV Analysis, conclusion and further developments.

The experimental results presented in Figure 4 and 5 are related to the dependence of the ion multiplicity M of emitted molecules from the target surface with the energy δE_{in} deposited "close to the surface" by the incident ions. The probability for the emitted particles to be ionized is dependent on the species. Therefore, M may be not representative of the overall emission (sputtering yield Y or total mass emitted per incident ion impact).

We have varied δE_{in} using two very different approaches:

A) by changing the ion velocity v_{in} and its charge state Q_{in}. With this approach, we vary the "local" contribution δE_{loc} in the surface disordered layer (from where the ions are emitted) together with the "distant" contribution δE_{Ge} from the crystal substrate, $\delta E_{in} = \delta E_{loc} + \delta E_{Ge}$ (a 70% variation of δE_{in} is achieved, see ζ_{in} in table 1,).

B) in channeling geometry, for given Q_{in} and v_{in}, by selecting special trajectories in the crystal through a selection of ΔE and Q_{out} values. Here, δE_{loc} is kept constant and δE_{Ge} is varied (typically by one order of magnitude). The specific contribution of δE_{loc} to <M> may be estimated from curves such as that of figure 5, by extrapolating <M> at zero substrate total energy loss (for example, $<M(\delta E_{Ge} = 0)>$ is close to 1 in figure 5).

All our experimental results show a rather surprisingly slow dependence of <M> as a function of δE_{Ge} when using procedure *B)*, (in particular, see figure

5, at high δE_{Ge} when <M> is essentially governed by δE_{Ge}). On the contrary, when using procedure A, we find a $(Q_{in}/v_{in})^p$ dependence for <M> in agreement with the literature. Another striking feature (see table 1) is that <M> increases when the incident beam is channeled. Finally, when considering the shape of the distribution of M, the probabilities P_n for high n (typically n >5), are small, but (see figure 4), they exhibit remarkably strong dependences with δE_{Ge}.

However, all these results suggest that the parameter M, as measured by the LAG detector, represents only one particular aspect of very complex processes. M is related to the total matter emitted per impact through complex physical processes: the (small) probability for an emitted molecule to be ionized, the probability for that molecule to be excited (electronic and vibrational excitation) and to break into two or more fragments, ionized or not, the distance from the accelerating grid where fragmentation occurs (related to he mean life time of the excited molecule) etc...

The mass spectra measured by the LAG exhibit a continuous background, which is the signature of fragmentation of large mass molecular ions. When fragmentation occurs between the target surface and the grid, the TOF analyzes a hypothetical mass which is neither that of the fragment nor that of the parent molecular ion. Indeed, the mass spectrum when conditioned by large M values exhibits mainly this background of undefined masses. Moreover, we have assumed that the LAG efficiency η is constant, which may not be the case for low velocity fragments (see §II.2). The observed differential effect involving enhanced fragmentation probabilities (see fig. 4) may hence be underestimated.

Keeping in mind the above considerations, one may analyze the experimental results as follows.

a) Our experimental results confirm the existence of a "depth effect". The relative influence of this effect as compared to the "local effect" (energy deposited very close to the emission location) depends on the energy loss below the sputtered layer. This dependence can be studied using the channeling technique over a wide range (from values of δE_{Ge} about twice smaller up to ten times larger than the energy deposit in random geometry).

b) It may be shown using Monte-Carlo simulations, that for the Pb aligned beams, the mean value $<\delta E_{Ge}>_{[110]}$ of the energy deposited close to the crystal surface, averaged over all the ions of the beam and over a few tens of nanometers, is typically of the order of $0.9\times<\delta E_{Ge}>_{Random}$. The fact that <M> increases slightly when changing from random to [110] alignment shows that the small fraction (10 to 20%) of ions with high S_{in} (grazing trajectories with respect to [110] rows) do more than to compensate the lowering of the multiplicity associated to the 80-90% ions experiencing low S_{in}.

c) We consider now the M distributions of figure 4 obtained for [110] alignment with ΔE selection (open circles and open squares). The increase by nearly two orders of magnitude of P_n for high n values when changing from very low $E_\perp$ to high $E_\perp$ is the signature of the dominant role of fragmentation at high M and of the very steep dependence of excitation of primary emitted molecular ions with S_{in}.

In order to get more insight into the relation between ion emission and energy deposition, several studies, not presented here, are in progress:

i) Study of the ion emission yield for given emitted species (with given mass *m*), in particular, mass peaks that receive no contribution from fragmentation (no background). Preliminary results show, as expected, that for well identified mass peaks, the ion emission yield varies more slowly with ΔE than when considering the whole emission yield.

ii) Study of the overall well identified ions emitted per ion impact (i.e. with no background of unidentified masses).

iii) Monte-Carlo simulations of the ion trajectories in Ge in order to relate the energy δE_{Ge} deposited close to the entrance surface (or S_{in}) to the total energy loss ΔE as measured by SPEG. Using such simulations, one might directly relate $<M>$ in figure 5 to $(\delta E_{Ge} + \delta E_{loc})$ rather than to ΔE.

iv) Detailed analysis of the influence of the variation of the charge state of the incident ions with depth, Q(z), for Pb^{28+} and Pb^{56+}. The analysis may also be performed with the help of Monte-Carlo simulations.

Further experiments in Ge or other materials could also bring valuable information:

v) Study of the ion emission as a function of the angle between the beam and the axis direction. In such experiments, the spatial repartition of δE_{Ge} close to the surface is varied as a function of depth z (the flux map is varied). This may give access to the depth scale z_d contributing to surface emission (in the literature [7], information on the "depth effect" was obtained through the variation of Q(z) in the solid; here Q may be kept constant).

vi) Study as a function of velocity for two ions with the same energy loss rate in random conditions but with “low” and “high” velocities (on opposite sides of the maximum of the stopping power curve S(v)).

References.

[1] C. Cohen and D. Dauvergne, Nucl. Instr. Meth. B 225 (2004) 40.
[2] I. Vickridge, A. L'Hoir, J. Gyulai, C. Cohen, F. Abel, Europhys. Lett. 13 (1990) 635.
[3] A. L'Hoir, S. Andriamonje, R. Anne, N.V. De Castro Faria, M. Chevallier, C. Cohen, J. Dural, M.J. Gaillard, R. Genre, M. Hage-Ali *et al.*, Nucl. Instr. Meth. B 48 (1990) 145.
[4] A. L'Hoir, L. Adoui, F. Barrué, A. Billebaud, F. Bosch, A. Bräuning-Demian, H. Bräuning, A. Cassimi, M. Chevallier, C. Cohen *et al.*, Nucl. Instr. Meth. B 245 (2006) 1.
[5] M. Bender, H. Kollmus and W. Assmann, Nucl. Instr. Meth. B 256 (2007) 387–391.
[6] L. Bianchi, B. Fernandez, J. Gastebois, A. Gillibert, W. Mittig, and J. Barrette, Nucl. Instr. Meth. A 276 (1989) 509.
[7] K. Wien, O. Becker, W. Guthier, S. Della-Negra, Y. Le Beyec, B. Monart, K.G. Standing, G. Maynard, C. Deutsch, Int. J. of Mass Spectr. and Ion Processes, 78 (1987) 273.
[8] S. Della-Negra, Y. Le Beyec, B. Monart, K. Standing, K. Wien, Nucl. Instr. and Meth. B 32 (1988) 85.
[9] J.F. Ziegler, J.P. Biersack, U. Littmarck, The Stopping and Ranges of Ions in Matter, Vol. 1, Plenum, New York.
[10] S. Revillon, Y. J. Chabal, F. Amy, A. Kahn, Appl. Phys. Lett. 87 (2005) 253101.
[11] S. Sun, Y. Sun, Z. Liu, S.I. Lee, S. Peterson, P. Pianetta, Appl. Phys. Lett. 88 (2006) 021903.
[12] G. Amsel, J.P. Nadai, E. D'Artemare, D. David, E. Girard, J. Moulin, Nucl. Instrum. Meth. 92 (1971) 481.
[13] F. Barrué, M. Chevallier, D. Dauvergne, R. Kirsch, J.-C. Poizat, C. Ray, L. Adoui, A. Cassimi, H. Rothard, M. Toulemonde *et al.*, Phys. Rev. A 70 (2004) 032902.
[14] S. Bouneau, P. Cohen, S. Della Negra, D. Jacquet, Y. Le Beyec, J. Le Bris, M. Pautrat, R. Sellem, Rev. Sci. Instrum. 74 (2003) 1.
[15] S. Bouneau, S. Della-Negra, D. Jacquet, Y. Le Beyec, M. Pautrat, M.H. Shapiro, T.A. Tombrello, Phys. Rev. B 71 (2005) 174110.
[16] A. Brunelle, S. Della-Negra, J. Depauw, H. Joret, Y. Le Beyec, K. Wien, Rad. Effects and Defects in Solids 110 (1989) 85.
[17] M. Most, K. Wien, A. Brunelle, S. Della Negra, J. Depauw, D. Jacquet, M. Pautrat, Y. Le Beyec, Nucl. Instr. and Meth. B 168 (2000) 203.
[18] S. Della Negra, Y. Le Beyec, B. Monart, K. Standing, K. Wien, Phys. Rev. Lett. 58 (1987) 17.